SYSTEMS ANALYSIS OF TRANSCRIPTIONAL DATA PROVIDES INSIGHTS INTO MUSCLE'S BIOLOGICAL RESPONSE TO BOTULINUM TOXIN

KAVITHA MUKUND, MS,[1] MARGIE MATHEWSON, MS,[2] VIVIANE MINAMOTO, PT, PhD,[4,5] SAMUEL R. WARD, PT, PhD,[4,5,6] SHANKAR SUBRAMANIAM, PhD,[1,2,3] and RICHARD L. LIEBER, PhD[2,4,6]

[1] Bioinformatics and System Biology Graduate Program, University of California San Diego, La Jolla, California, USA
[2] Department of Bioengineering, University of California San Diego, La Jolla, California, USA
[3] Department of Cellular and Molecular Medicine, University of California San Diego, La Jolla, California, USA
[4] Department of Orthopaedic Surgery, University of California San Diego, 9500 Gilman Drive, MC0863, La Jolla, California 92093-0863, USA
[5] Department of Radiology, University of California San Diego, La Jolla, California, USA
[6] Veterans Affairs San Diego Healthcare System, La Jolla, California, USA

Accepted 13 February 2014

ABSTRACT: *Introduction*: This study provides global transcriptomic profiling and analysis of botulinum toxin A (BoNT-A)–treated muscle over a 1-year period. *Methods*: Microarray analysis was performed on rat tibialis anterior muscles from 4 groups ($n = 4$/group) at 1, 4, 12, and 52 weeks after BoNT-A injection compared with saline-injected rats at 12 weeks. *Results*: Dramatic transcriptional adaptation occurred at 1 week with a paradoxical increase in expression of slow and immature isoforms, activation of genes in competing pathways of repair and atrophy, impaired mitochondrial biogenesis, and increased metal ion imbalance. Adaptations of the basal lamina and fibrillar extracellular matrix (ECM) occurred by 4 weeks. The muscle transcriptome returned to its unperturbed state 12 weeks after injection. *Conclusions*: Acute transcriptional adaptations resemble denervated muscle with some subtle differences, but resolved more quickly compared with denervation. Overall, gene expression across time correlates with the generally accepted BoNT-A time course and suggests that the direct action of BoNT-A in skeletal muscle is relatively rapid.

Muscle Nerve **50**: 744–758, 2014

Skeletal muscle contraction is controlled by impulses received from the central nervous system via the neuromuscular junction (NMJ). In cases where skeletal muscle function is impaired due to altered activity of nerve impulses, as in movement disorders such as cerebral palsy (CP), it can be advantageous to suppress muscle contraction by reducing NMJ activity. Signal reduction can be achieved by physically decoupling the muscle and nerve by selective dorsal rhizotomy,[1] or through the use of chemical agents such as neurotoxins.[2] One such neurotoxin in common clinical use is botulinum toxin A (BoNT-A), which has applications ranging from decreasing spasticity, tics, and tremors, to managing pain and controlling glandular secretions.[3]

BoNT-A is 1 of 7 serotypes produced by *Clostridium botulinum* that functions to reversibly paralyze muscle by affecting the NMJ. BoNT-A reduces presynaptic acetylcholine (ACh) release by specifically cleaving a SNARE protein, SNAP25, required for its exocytosis. BoNT-A–induced neuromuscular block causes physical and physiological changes to the NMJ and skeletal muscle fiber.[4,5] Experimental studies have shown that muscle reinnervation via neuronal sprouting begins immediately after injection, with control slowly reverting back to the parent terminal over time.[6,7] It has also been observed that, during this time, skeletal muscle is characterized by reduced fiber size, paresis, and atrophy,[8] until it gradually regains functionality. When used as a therapeutic agent in disorders such as CP, BoNT-A is administered by intramuscular injection repeatedly over extended periods of time. Although clinical experience has demonstrated that the injection effects last 3–6 months,[9] there is not yet a cohesive temporal picture or a clear understanding of underlying muscle functional and transcriptional regulation. Although the effects of BoNT-A treatments in skeletal muscle have been studied extensively experimentally,[4,7,10] to the best of our knowledge, only a single genomic study was published that focused on certain genes associated with BoNT-A action in skeletal muscle.[11] In contrast, we now report a complete systems analysis of the BoNT-A–treated skeletal muscle transcriptome over a period of 1 year, with the goal of understanding the underlying biological response to BoNT-A and the

Additional Supporting Information may be found in the online version of this article.

Abbreviations: ACh, acetylcholine; ADP, adenosine triphosphate; ATP, adenosine triphosphate; BH, Benjamini–Hochberg; BoNT-A, botulinum neurotoxin A; CP, cerebral palsy; DHPR, dihydropyridine receptors; ECC, excitation–contraction coupling; ECM, extracellular matrix; GCRMA, gene chip robust multi-array average; GEO, Gene Expression Omnibus; IGF, insulin-like growth factor; MRF, myogenic regulatory factor; MuSK, muscle-specific tyrosine kinase; nAChR, nicotinic acetylcholine receptor; NF-kappaB, nuclear factor–κB; NMJ, neuromuscular junction; qPCR, real-time quantitative polymerase chain reaction; ROS, reactive oxygen species; RYR, ryanodine receptor; SLC, solute carrier; SR, sarcoplasmic reticulum; TA, tibialis anterior

Key words: botulinum toxin A; cross-sectional study; microarray gene expression; neurotoxin; skeletal muscle; time course

This study was financially supported by grants from the Department of Veterans Affairs (RX000670 to R.L.); the National Institutes of Health (R24HD050837 to R.L. and AR057013 to S.W.), Allergan, Inc. (to R.L.); the National Heart, Lung, and Blood Institute (HL087375-02, HL106579, and HL108735 to S.S.); and the National Science Foundation (STC-0939370 to S.S.).

Correspondence to: R.L. Lieber; e-mail: rlieber@ucsd.edu or S.Subramaniam; e-mail: shankar@ucsd.edu or S.Subramaniam; e-mail: shankar@ucsd.edu

Published online 18 February 2014 in Wiley Online Library (wileyonlinelibrary.com). DOI 10.1002/mus.24211

relationship between transcriptional and functional changes associated with its reversible paralysis. We analyze our results in the context of "physiological families" of skeletal muscle, as presented recently.[12,13] Thus, the primary goal for this study was 2-fold: (1) to create a documented model for global transcriptional changes that occur with neurotransmitter blockade using BoNT-A in skeletal muscle; and (2) to gain insights into the biological basis for adaptation and recovery of muscle after BoNT-A treatment.

METHODS

Animals. All procedures were performed with the approval of the institutional animal care and use committee of the University of California, San Diego. Mature male Harlan Sprague-Dawley rats (age 3 months, weight 399 ± 3.05 g) were given a single 100-μl injection in the tibialis anterior (TA) muscle with either saline or saline with 6 U/kg BoNT-A (Botox® / Onabotulinum toxin A; Allergan, Irvine, California). At 1, 4, 12, and 52 weeks after injection, rats were euthanized by intracardiac pentobarbital sodium (0.5 ml of 390-mg/ml solution) injection. Maximum isometric contraction strength was measured for all rats before euthanasia, as described previously.[14] After the animals were euthanized, bilateral TA muscles were excised, weighed, and snap-frozen in isopentane cooled with liquid nitrogen (−159°C). All samples were stored at −80°C for further analysis.

Hydroxyproline Assay. A modified version of the hydroxyproline assay[15] was used to determine collagen content. Briefly, muscles were hydrolyzed at 110°C overnight in hydrochloric acid, then methyl red was added and samples were pH adjusted. Chloramine T and *p*-diaminobenzaldehyde were added sequentially to the samples, which were then incubated for 30 minutes at 60°C. A standard curve was determined, and samples were read at 550 nm and 558 nm.

RNA Preparation. Samples were prepared for 5 groups ($n = 4$/group) that included tissue from TAs of BoNT-A–injected rats at 1, 4, 12, and 52 weeks after injection and control tissue from the contralateral TA of saline-injected rats euthanized at 12 weeks. RNA was extracted with Trizol (Invitrogen, Carlsbad, California) and RNeasy (Qiagen, Valencia, California). Briefly, 30 mg of frozen tissue was mixed with 0.5 ml of Trizol and homogenized at 4°C in a bullet blender (Next Advance, Inc., Averill Park, New York). The homogenate was mixed with 100 μl of chloroform, and samples were incubated for 2 minutes at room temperature and spun at 4°C for 15 minutes. The aqueous portion was removed and mixed with equal amounts of 70% ethyl alcohol. The solution was then washed through an RNeasy spin column, incubated for 15 minutes with RNAse-free DNAse (Qiagen), washed 3 times, and eluted according to the manufacturer's instructions. Absorbance was measured at 260 nm to determine RNA concentration, and the 260/280-nm absorbance ratio was calculated to determine RNA purity. RNA was reverse-transcribed into cDNA using a synthesis system (SuperScript First-Strand Synthesis System; Life Technologies, Grand Island, New York).

Microarray Data Collection. Microarrays (RG-230 2.0; Affymetrix, Santa Clara, California) were used for analysis of all samples. The Cancer Center Microarray Shared Resource (University of California, San Diego) provided RNA processing and quality control using the GS FLX System (Roche Diagnostic Corp., Basel, Switzerland).

Real-Time Quantitative Polymerase Chain Reaction. Real-time quantitative PCR (qPCR) was conducted to validate expression of 8 genes (*Chrna1*, *Myl3*, *Sln*, *Myog*, *Aqp4*, *Runx1*, *Scd1*, *Atp1b4*) with cDNA prepared from RNA samples used for microarray analysis. We also quantified the expression of muscle-specific tyrosine kinase (MuSK) receptor through qPCR as it was undetectable at any time-point on our gene chip. RNA was reverse-transcribed into cDNA using the synthesis system (SuperScript First-Strand). Samples were diluted 1:100, and qPCR was performed using KAPA SYBR FAST Master Mix (Kapa Biosystems, Woburn, Massachusetts) and the Eppendorf Mastercycler System (Eppendorf, Hamburg, Germany). Primers for *Chrna1*, *Sln*, *Myl3*, *Myog*, *Aqp4*, *Runx1*, and *GAPDH* were designed in Oligo 6.8 (Molecular Biology Insights, Cascade, Colorado, and Allele Biotechnology, San Diego, California), whereas those for *Scd1*, *MuSK*, and *Atp1b4* were ordered pre-made from Integrated DNA Technologies (Coralville, Iowa). Primer sequences for these genes are listed in Table 1.

A temperature gradient was used to determine the optimal reaction temperature for each primer based on the DNA melting temperature curve and single product production on an agarose gel. Samples were run in triplicate using the following protocol: samples were heated to 95°C for 2 minutes; then run through 40 cycles of heating at 95°C for 15 seconds, cooling to 55°C for 15 seconds, and heating for 20 seconds to the optimal primer temperature determined by the temperature gradient described above. The triplicate results of each gene from qPCR data were normalized with respect to the housekeeping gene, *GAPDH*. Fold change was computed in accordance with a previous publication.[16]

Microarray Data Preprocessing. Expression data were preprocessed using software available through

Table 1. List of forward and reverse strand primer sequences that were utilized for validation of gene expression using qPCR.

Gene	Forward sequence	Reverse sequence
Chrna1	*TACTTGAATCCTTTCGCGCT*	*CTTAACCGCTGAGCCATCTC*
Sln	*TGGTGTGCACTCAGAAGTCC*	*TGAGGAGCACAGTGATCAGG*
Myl3	*AATCCTACCCAGGCAGAGGT*	*CATATGTGCCCGTGTCTTTG*
Myog	*ACCAGGAGCCCCACTTCTAT*	*TTACACACCTTACACGCCCA*
Aqp4	*GCATGTGATCGACATTGACC*	*GTGAAACAAGAAACCCGCAT*
Runx1	*TAACCCTGCCTGGGTGTAAG*	*GGACTCGGATCTTCTGCAAG*
GAPDH	*AGACAGCCGCATCTTCTTGT*	*TGATGGCAACAATGTCCACT*

R[17] and Bioconductor.[18] Gene chip robust multi-array average (GCRMA) was employed for normalizing expression using the "gcrma" function available through the GCRMA package.[19] All raw .CEL files along with GCRMA-normalized data are available through Gene Expression Omnibus (GEO),[20] accession GSE52350. Outlier samples were those with average intersample correlation <2 standard deviations (SD) below the mean. A single array at 1 week (3.4 SD below mean) was removed. Annotation files for RG 230 2.0 (GPL 1355) were downloaded from GEO. Multiple probes were accounted for using the "collapseRows" function in R's WGCNA library.[21] All probes with missing ENTREZ gene identifiers were excluded from this study. Based on this processing, we obtained a final reduced data set containing log2-based normalized expression values of 13,751 genes across 19 samples.

Differential Analysis through Pairwise Comparisons. Pairwise comparison between every time-point BoNT-A injected vs. saline was performed using Cyber-T[22] Bayes regularized analysis for 2-sample unpaired data, with a confidence interval of 8. This study utilized control tissue from saline-injected rats 12 weeks after injection for all pairwise comparisons, in contrast to using age-matched controls. Rats from this time were considered adult animals, representative of rats from the other time-points in the study. Previous studies have shown that skeletal muscle glucose uptake[23] and muscle protein expression[24] changes little among rats until they reach >18 months of age. Because all our rats were within this age group, we considered it acceptable to perform pairwise comparison using a control from a single time-point. Fold change for each gene was computed as the difference in mean log2-based expression between treated and control samples. Genes with a log2-based fold of >1 and a Benjamini–Hochberg (BH) $P < 0.05$ were identified as being significantly differentially expressed, as presented in Table S1a (refer to Supplementary Material, available online).

Enrichment Analysis. DAVID[25] was used to identify enrichment of genes (categories: GO_BP_FAT and KEGG_PATHWAYS) as shown in Table S1b (online).

RESULTS

Differential Gene Expression over Time. Gene expression changed dramatically during the experimental time period. Table 2 summarizes the number of genes that were identified as being differentially regulated at each time-point. Consistent with previous studies, pairwise analysis revealed that muscle is transcriptionally hyperactive, with dramatic transcriptional changes at 1 week (compared with 4, 12, and 52 weeks). Visual analysis of differentially regulated genes suggests that the bulk of regulation occurs at 1 week, with a large fraction of genes (1718 of 1989) being exclusively and significantly regulated at this time (Fig. 1). As expected, the genes regulated at 1 week cover a wide spectrum of functions, such as stabilizing the NMJ, sarcomeric contraction, and muscle metabolism. Of the 113 genes regulated exclusively at 4 weeks, most were associated with extracellular matrix (ECM) and collagen fibril organization (Table S1b, online). No genes were regulated significantly across the entire course of the study.

Systems Analysis of Differential Expression in Skeletal Muscle. In contrast to using traditional ontology enrichment to analyze transcriptional regulation, we systematically categorized and analyzed differentially expressed genes in the novel framework of "physiological networks" specifically identified in skeletal muscle from 2 previous studies.[12,13] Wang *et al.*[13] identified families of genes based on 4 major functions occurring in skeletal muscle, namely mechanical, metabolic, excitation–contraction coupling, and signaling, whereas Smith *et al*[12] characterized the physiology of the muscle into 8 distinct "networks" required for its functioning. Taken together, these models have identified gene

Table 2. Summary of differentially regulated genes identified at each time (with respect to saline injected muscle, BH P<0.05).

Time (in weeks)	Differentially expressed	Upregulated	Downregulated
1	1989	1183	806
4	372	303	69
12	32	19	13
52	32	19	13

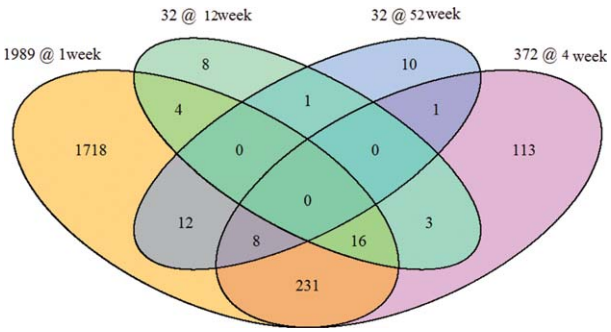

FIGURE 1. A 4-way Venn diagram depicting the distribution of differentially expressed genes across all pairwise comparisons and counts of overlapping genes between multiple pairwise comparisons. The count within each shaded area represents the number of differentially expressed genes identified in common between time-points. For example, 231 genes were differentially expressed at both 1 and 4 weeks.

networks that are crucial for normal skeletal muscle function and homeostasis.

Utilizing these models to guide our analyses, we derived a systems view of the regulation underlying skeletal muscle after BoNT-A treatment. Based on our data set, transcriptional activity of muscle can be grouped into 7 networks: (1) neuromuscular junction; (2) excitation–contraction coupling (ECC); (3) muscle contraction; (4) energy metabolism and mitochondrial biogenesis; (5) ECM; (6) oxidative stress; and (7) muscle atrophy and recovery (Fig. 2 and Table S2, available online). Each of these networks can be considered in their physiological context in light of the genes measured.

Neuromuscular Junction. Expression changes at the NMJ are presented graphically in Figure 3. Consistent with previous experimental studies, BoNT-A injection leads to rapid disruption and repair of the NMJ. Genes encoding postsynaptic proteins were detected, including the adult nAChr subunits *Chrna1*, *Chrnd*, *and Chrne*, as well as the developmental subunit *Chrng*, which is usually only expressed in humans prior to week 33 of gestation. The co-receptor for Agrin, *Lrp4*, and *Emb* and linker protein *Rapsn* were all upregulated. *Chrna1* and *Emb* were upregulated until 4 weeks. Two immature isoforms of Na^{2+} and K^{+} channels, *Scn5a* and *Kcnn3*, were upregulated significantly at 1 week. Genes selectively involved with the synaptic basal lamina, including *Lama5*, *Col4a5*, and *Nid2*, were upregulated only at 4 weeks.

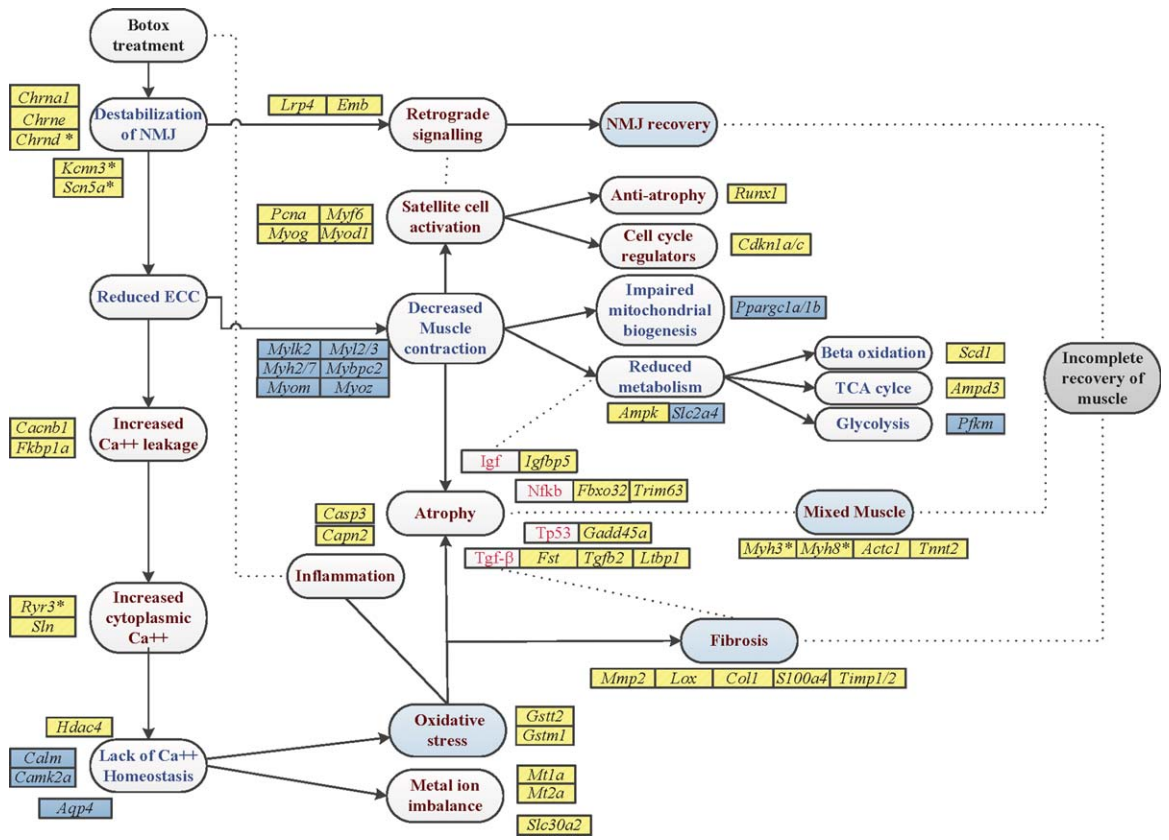

FIGURE 2. Overview of transcriptional changes occurring in adult skeletal muscle after BoNT-A treatment. Functional changes represented in blue boxes show associated gene expression until 4 weeks after injection. Genes in yellow boxes exhibit upregulation, and genes in blue boxes exhibit downregulation. Genes identified with an asterisk represent immature muscle isoforms. Signaling pathways are indicated with red text. Dotted lines indicate association, and arrows indicate a cause–effect relationship.

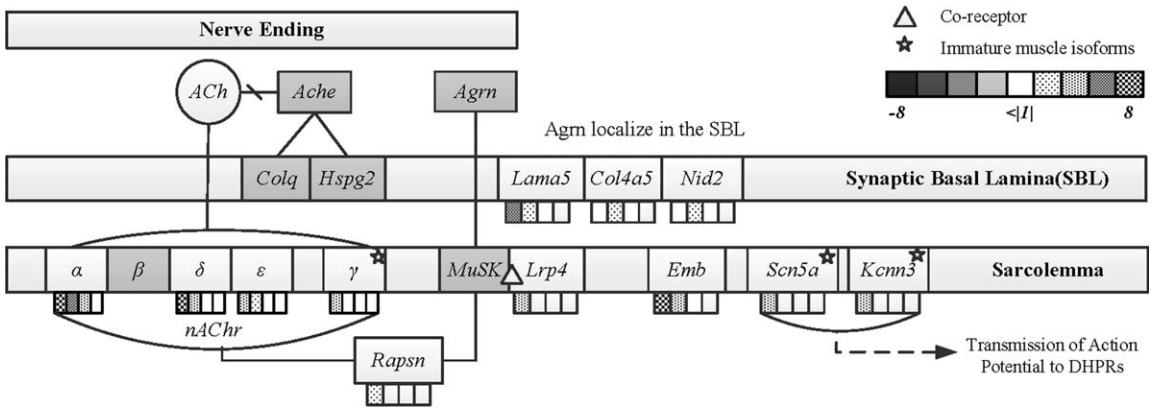

FIGURE 3. Expression of genes involved in the neuromuscular junction over time. Each box has 4 partitions representing the time-points at which samples were obtained. Each box represents the fold changes observed and is colored according to the legend. Genes that are not represented in the microarray or identified as differentially expressed are presented in gray. Solid lines indicate either an interaction among genes or an association between genes.

Excitation–Contraction Coupling. Genes involved in ECC and maintenance of calcium homeostasis, such as ion pumps and ion channels, were differentially regulated, especially at 1 week (Fig. 4 and Table S2, online). *Cacnb1* (an L-type voltage-gated Ca^{2+} channel) and *Fkbp1a* (an *Ryr1* binding protein) were upregulated. Sustained and significant upregulation of sarcoplasmic Ca^{2+} handler sarcolipin (*Sln*) occurred up to 12 weeks. *Jph1* and genes required to modulate cytosolic Ca^{2+} levels, including *Pde4d*, *Calm3*, and *Camk2a*, were downregulated at 1 week.

Aqp4 was the most strongly downregulated gene at 1 week. Several K^+ ion channels, such as *Kcnc1*, *Kcnab1*, and *Kcnj11*, and ion pumps, such as *Atp1b1* and *Atp1b2* were also downregulated.

Muscle Contraction and Activation. Muscle contraction requires coordinated effort between the contracting sarcomeres and cytoskeletal framework. There is a general downregulation of genes associated with activating sarcomere contraction in fast fibers, particularly 1 week after injection ((Fig. 4 and Table S2, online). These include tropomyosin (*Tpm3*, *Tpm2*), troponins (*Tnnc1*, *Tnnt1*, *Tnni1*), and tropomodulin (*Tmod1*), and genes that encode proteins associated with the sarcomeric contractile apparatus, such as myosin light chains (*Myl2*, *Myl3*), Myl kinases (*Mylk2*), *Mybpc2*, and myosin heavy chains (*Myh2*, *Myh7*). There was a significant downregulation of the M-line structural proteins, including myomesins (*Myom1 and Myom2*), *Z*-disk–associated proteins such as *Actn3*, *Myot*, myozenins (*Myoz1*, *Myoz2*), and *Ldb3*. Cytoskeletal proteins *Ank1*, *Sgc*, *and LARGE* were downregulated, whereas cytoskeletal proteins required to increase sarcolemmal stability were upregulated (*Csrp3*, *Dysf*, *Dtna*, *Flnc*, *Lmna*). We also observed

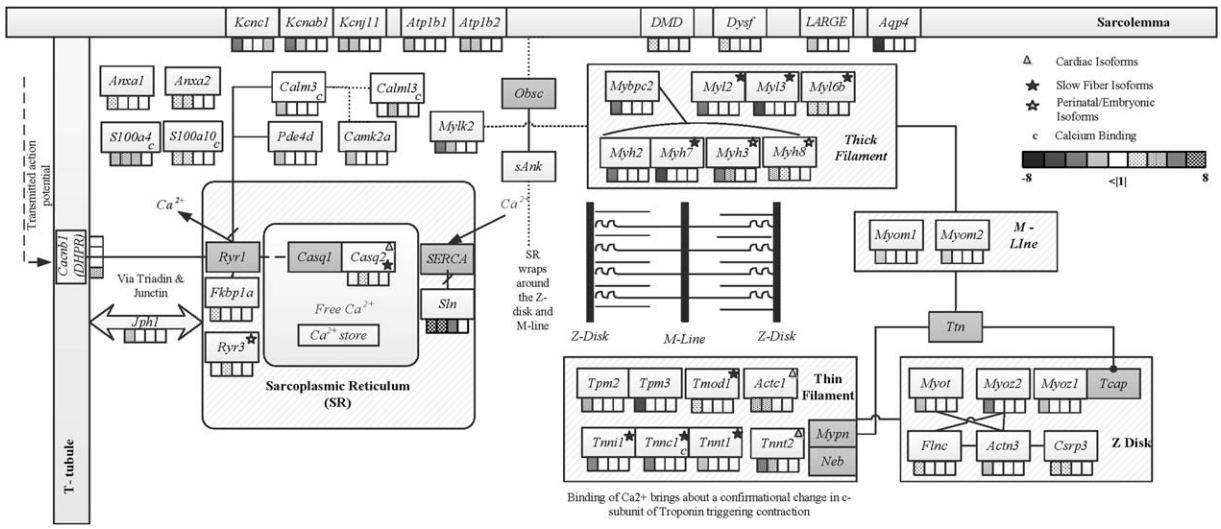

FIGURE 4. Expression of genes involved in excitation–contraction coupling and muscle contraction after BoNT-A injection. Expression levels are depicted as described in Figure 3.

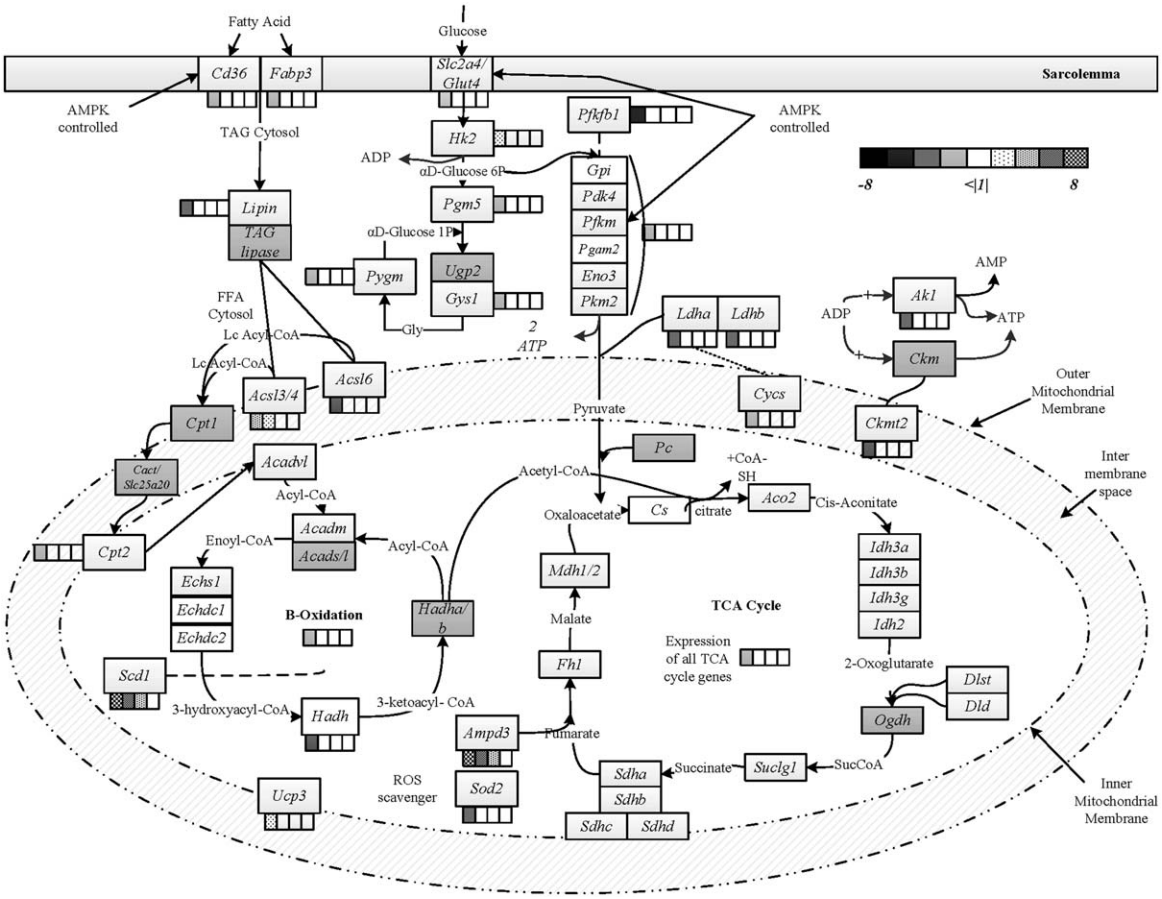

FIGURE 5. Mitochondrial metabolism in skeletal muscle and a depiction of the expressed fold changes of genes involved. Expression levels are depicted as described in Figure 3.

strong upregulation of a muscle-specific calcium-handling protein, *Ankrd1*, up to 4 weeks. Upregulation of certain cardiac isoforms, such as *Actc1*, *Myl6b*, and *Tnnt2*, along with immature isoforms normally absent from adult muscle (*Myh3*, *Myh8*), was also observed. Consistent with this observation was the appearance of developmental myosin isoforms in 14% of the 1-week and 1-month injected muscles, but not in control muscle.

Energy Metabolism and Mitochondrial Biogenesis. Genes involved in energy metabolism, specifically mitochondrial energy production from glycolysis and β-oxidation, were downregulated significantly 1 week after injection (Fig. 5 and Table S2, online). The glucose transporter, *Glut4/SLc2a4*, and glycolysis intermediates and enzymes, *Pgm5*, *Gys*, *Pygm*, *and Pfkfb1*, were downregulated at 1 week. Other enzymes involved in generation of pyruvates acting in the cytosol, such as *Gpi*, *Pfkm*, *Pgam2*, *Eno3*, *Pkm2*, *Pdk4*, *Ldha*, and *Ldhb*, were downregulated at 1 week. Enzymes involved in each step of the TCA cycle, including *Cs*, *Aco2*, *Idh2*, *Idha*, *Idhb*, *Idhg*, *Dlst*, *Dld*, *Suclg1*, *Sdha*, *Sdhb*, *Sdhc*, *Sdhd*, *Fh1*, *Mdh1*, and *Mdh2*, were downregulated. AMP deaminase (*Ampd3*), required for replenishing TCA cycle intermediates, was upregulated strongly.

Genes associated with β oxidation and lipid metabolism were downregulated. These included: fatty acid transporters *Cd36* and *Fabp3*; *Lipin-1* [required to break down triacylglycerol to free fatty acids (FFA)]; ATP-dependent enzymes required to convert FFA into long, medium, and short acyl-CoA esters (*Acadvl*, *Acsl6*, *Acss1*) and their transporters (*Cpt2*); *Hadh*; and *Echs1*, *Echdc1*, *and Echdc2*. Prolonged upregulation of stearoyl–coenzyme A desaturase 1 (*Scd1*) was observed for most of the study. Genes of the immediate adenosine triphosphate (ATP) replenishment system of muscle, *Ckmt2* and *Ak1*, were downregulated. Major energy/ATP availability sensor, AMPK α/β/γ (*Prkaa1*, *Prkag3*), was upregulated. Targets of AMPK, the peroxisome proliferator–activated receptor-γ (PPAR) cofactors, *Ppargc1a* and *Ppargc1b*, were downregulated.

Downregulation of solute carriers necessary for metabolism, such as several members of the mitochondrial phosphate transporter family (*Slc25–*

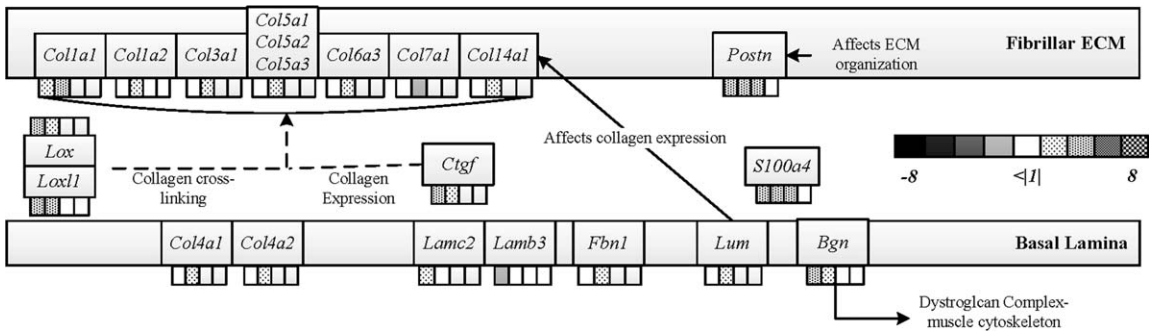

FIGURE 6. Diagram of fold changes of genes involved in the basal lamina and fibrillar ECM. Expression levels are depicted as described in Figure 3.

Slc25a23 in particular) and members of the monocarboxylate transporter subfamily (*Slc16–Slc16a3* in particular) was observed.

Changes to Extracellular Matrix. There was a general upregulation of ECM genes, particularly at 4 weeks after injection. Genes encoding proteins of the basal lamina, such as *Fbn1*, and its collagens (*Col4a1*, *Col4a2*, *Col8a1*), were upregulated (Fig. 6 and Table S2, online). Genes associated with the fibrillar ECM, including *Col1a1*, *Col1a2*, *Co114a1*, *Col3a1*, *Col5a1*, *Col5a2*, *Col5a3*, and *Col6a3*, and other ECM-associated genes, such as *Lum*, *Ctgf*, *Bgn*, and *Postn*, were upregulated. Enzymes *Lox* and *Loxl1*, involved in collagen cross-linking, were also upregulated. *S100a4*, a biomarker correlated with proliferation of fibroblasts, was upregulated through 12 weeks. Increased collagen at the protein level in samples from 4 weeks was also detected using the hydroxyproline assay (Fig. S1, online).

Oxidative Stress Response. The most striking change in expression of genes involved in oxidative stress was the global activation of chemoprotective and antioxidant genes, especially at 1 week, which involved the isoforms of glutathione *S*-transferase (*Gst*, specifically *Gstm1* and *Gstt2*), *Gpx3*, *Hmox*, *Nqo1*, *Aldh3a2*, *Txn1*, and metallothioneins (*Mt1a*, *Mt2a*). The mitochondrial reactive oxygen species (ROS) scavenger, *Sod2*, was downregulated at 1 week.

Muscle Atrophy and Recovery. After BoNT-A injection, muscle appears to activate conflicting cellular programs, showing simultaneous signs of breakdown and repair. Upregulation of myogenic regulatory factors (MRFs), *Myod1*, *Myog*, and *Myf6*, at 1 week, with a concomitant and drastic increase in 2 potent regulators of cell proliferation, *Cdkn1a* and *Cdkn1c*, was observed. These, in conjunction with activated *Pcna*, serve as markers of satellite cell activation in skeletal muscle. Signaling pathways active in BoNT-A–treated skeletal muscle are as follows (Fig. 7 and Table S2, online).

Transforming growth factor-beta (TGF-β) pathway: Several genes in the TGF-β pathway, including *Tgfb2*, *Fst*, *Myc*, *Ltbp1*, and early response factors downstream, *Junb* and *Fos*, were upregulated significantly up to 4 weeks. Small GTPases, *RhoA* and *RhoC*, downstream of the TGF-β pathway, were upregulated at 1 week with *Mstn* receptor *Acvr2b*, *Acvr1*, and a TF, *Atf4*, downregulated at 1 week. Interestingly, inhibitors of *Tgfb1*, such as *Smad7* and *Fkbp1a*, were upregulated at 1 week.

Nuclear factor–kappaB (NF-κB) signaling: Several genes, including *Traf2*, *Nfkb2*, and *Nfkbie*, and ubiquitin ligases downstream of the *NF-κB* pathway, *Atrogin1/Fbxo32 MuRF1/Trim63*, and *Casp3*, were upregulated at 1 week. Positive activators of the *NF-κB* pathway, such as *Ascc2* and *Litaf*, were also upregulated at 1 week.

MAPK signaling: Several members of the MAPK family were upregulated at 1 week, including *Mapk1*, *Mapk3*, *Map3k1*, *Map3k14*, *Map4k4*, and *Mapk1ip1*, as well as its downstream targets, such as *Eif4e2*, which initiates protein translation and activation of *Myod1*.

Insulin signaling: Although we found no significant regulation of *Igf1* in our study, several genes of this pathway were upregulated at 1 week, including *Igf1r*, *Igfbp5*, and *Shc*, and downstream, *Pik3r4* and *Akt1*. Regulation of *Igfbp5* and *Igf2* is observed at 4 weeks. *Glut4/Slc2a4* and *Irs1* were downregulated at 1 week.

ID signaling pathway: Inhibitor of DNA binding (ID) proteins *Id1*, *Id2*, *Id3*, and *Id4* were upregulated up to 4 weeks. This pathway is believed to play a role in repairing muscle.

TP53/cell cycle control: Activation of genes that may play a role in satellite cell proliferation and activation of apoptosis, including *Cdkn1a*, *Gadd45a*, *Pcna*, and *Myc*, were upregulated at 1 week.

VEGF pathway: Genes involved in angiogenesis, including *Vegfa*, *Vegfb*, angiopoietins (*Angpt1*, *Angpt2*), *Nos3*, *Rtn4*, and *Nrp1*, were downregulated at 1 week.

Transcriptional regulation of factors required for proteolytic degradation, such as Ca^{2+}-dependent calpains (*Capn2*, *Capn3*) and lysosomal

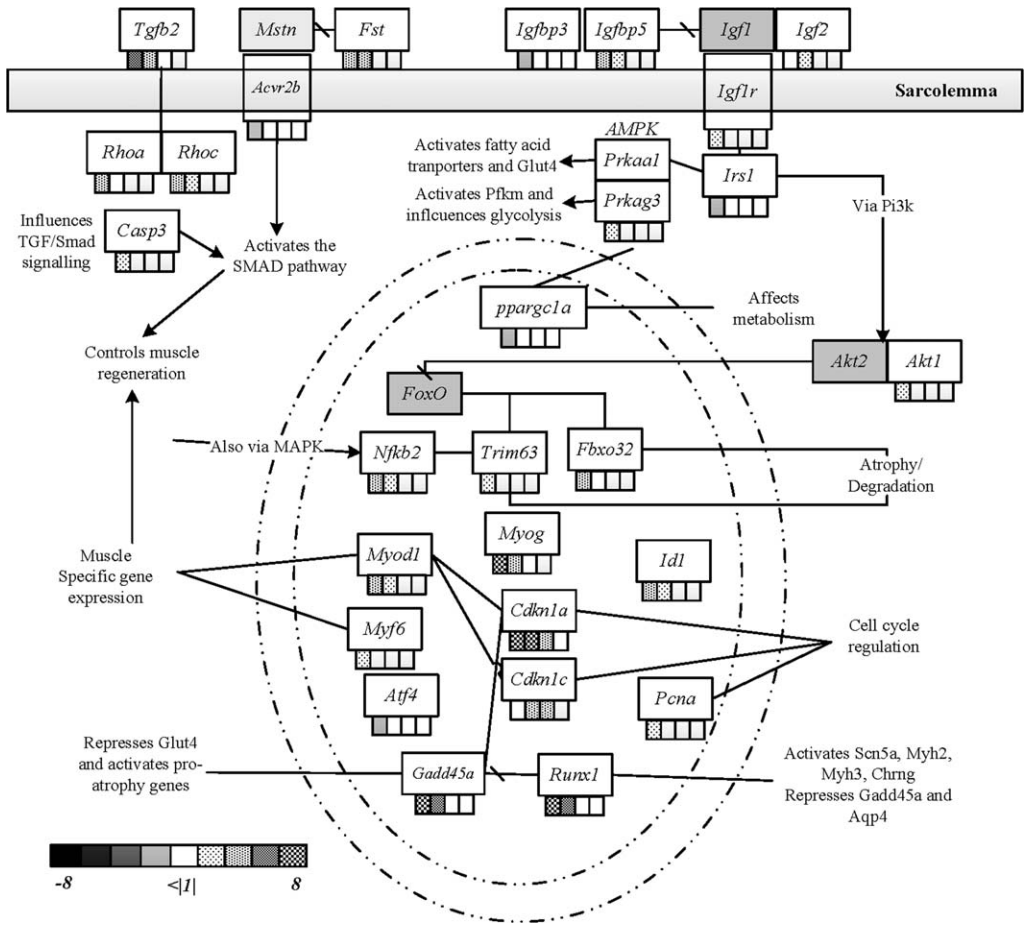

FIGURE 7. Illustration of a representative set of active transcription factors and signaling pathways involved in atrophy and muscle recovering from BoNT-A injection and their fold changes across time. A detailed list of genes is provided in Table S2 (available online). Expression levels are depicted as described in Figure 3.

cathepsins (*Ctsl1*), was seen. *Runx1*, a transcription factor that promotes anti-atrophic programs, was upregulated strongly up to 4 weeks.

Validation of Regulated Gene Expression Using qPCR. To validate the chip-based expression results, we performed qPCR on a subset of 8 relevant genes. Some have been highlighted previously as being active in skeletal muscle during atrophy, specifically after BoNT-A treatment, including *Myog*, *Chrna1*, *Sln*, and *Myl3*. Genes that were shown more recently to be active in atrophy/muscle recovery from atrophy include *Runx1*.[26] Genes that were ranked highly in our analyses with a demonstrated role in skeletal muscle include *Scd1* and *Aqp4*, and another with no known role in skeletal muscle, but highly ranked in our differential analysis, was *Atp1b4*. The average fold change of all genes was normalized with respect to *GAPDH*. Average fold change was computed with reference to the saline-injected samples. The trends seen in qPCR were similar to those computed through microarray differential analysis (Fig. 8). Quantitative correlation between relative gene expression levels from microarray data and qPCR (r^2) ranged from 0.74 to 0.99.

Correlation of Gene Expression with Muscle Function Postinjection. Because measurement of isometric contraction was made before and after BoNT-A injection on the same set of rats used for gene expression analysis, we could study the correlation over the time course of our experiment. We correlated isometric contraction strength postinjection with genes identified as significantly altered for the 1- and 4-week time periods (Table S1b, online). At 1 week, 72 genes were correlated positively and 37 genes were correlated negatively ($P < 0.05$) with contraction strength. These same 109 genes showed the opposite weak correlation (albeit non-significantly) with isometric force prior to injection (Fig. 9, left), suggesting that expression levels may be functionally significant. Positively correlated genes were enriched for skeletal muscle contraction and include genes such as *Chrna1*, *Myl2/3*, *Tnni1*, *Tnnc1*, *Lama5*, *Scn5a*, *Myoz2*, and *Tpm3* (Table S1b, online). Because a functional contractile apparatus is required for muscle contraction, it is not surprising that increasing

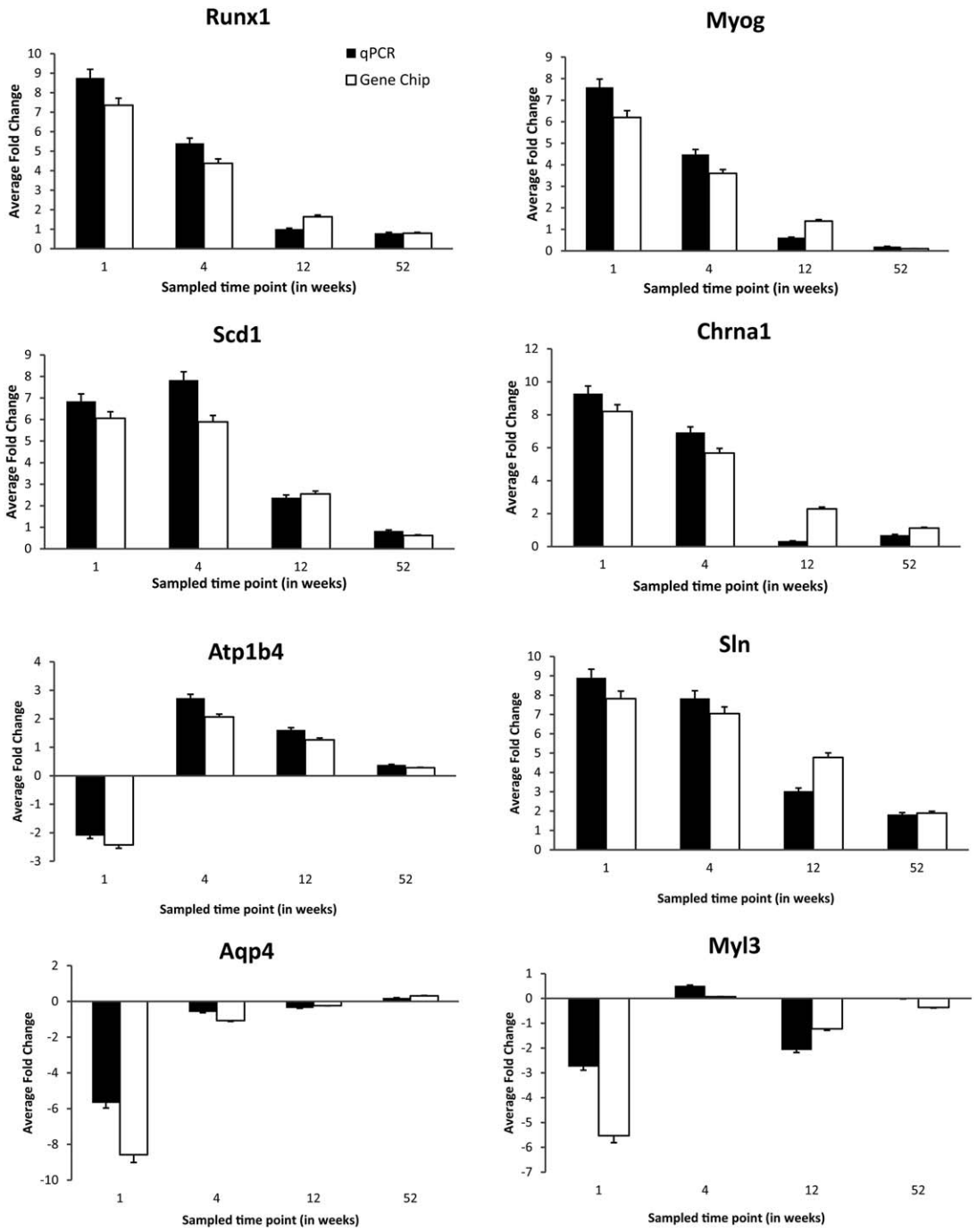

FIGURE 8. Fold changes observed based on the qPCR assay compared with the microarray data. Each plot shows a comparison between the gene's calculated average fold change (log2-based) with respect to control using qPCR and microarray analysis computed for each time-point.

expression of related genes may improve contraction strength after BoNT-A injection. At 4 weeks, we observed 15 genes correlating positively ($P < 0.05$) and 37 correlating negatively ($P < 0.05$; Fig. 9, right) with isometric force after injection. Negatively correlated genes were overrepresented for angiogenesis, cell death, and ECM (such as *Lox* and *Col1a1*) (Table S1b, online). Although it has been shown previously that fibrosis and ECM remodeling may lead to abnormal muscle function,[27] the link between angiogenesis and muscle force is less clear. These data may be indicative of still-injured muscle undergoing continued repair and regrowth at 4 weeks.

DISCUSSION

This study is a high-throughput analysis of global expression changes in BoNT-A–treated mammalian skeletal muscle over a period of 1 year (Fig. 2). Albeit

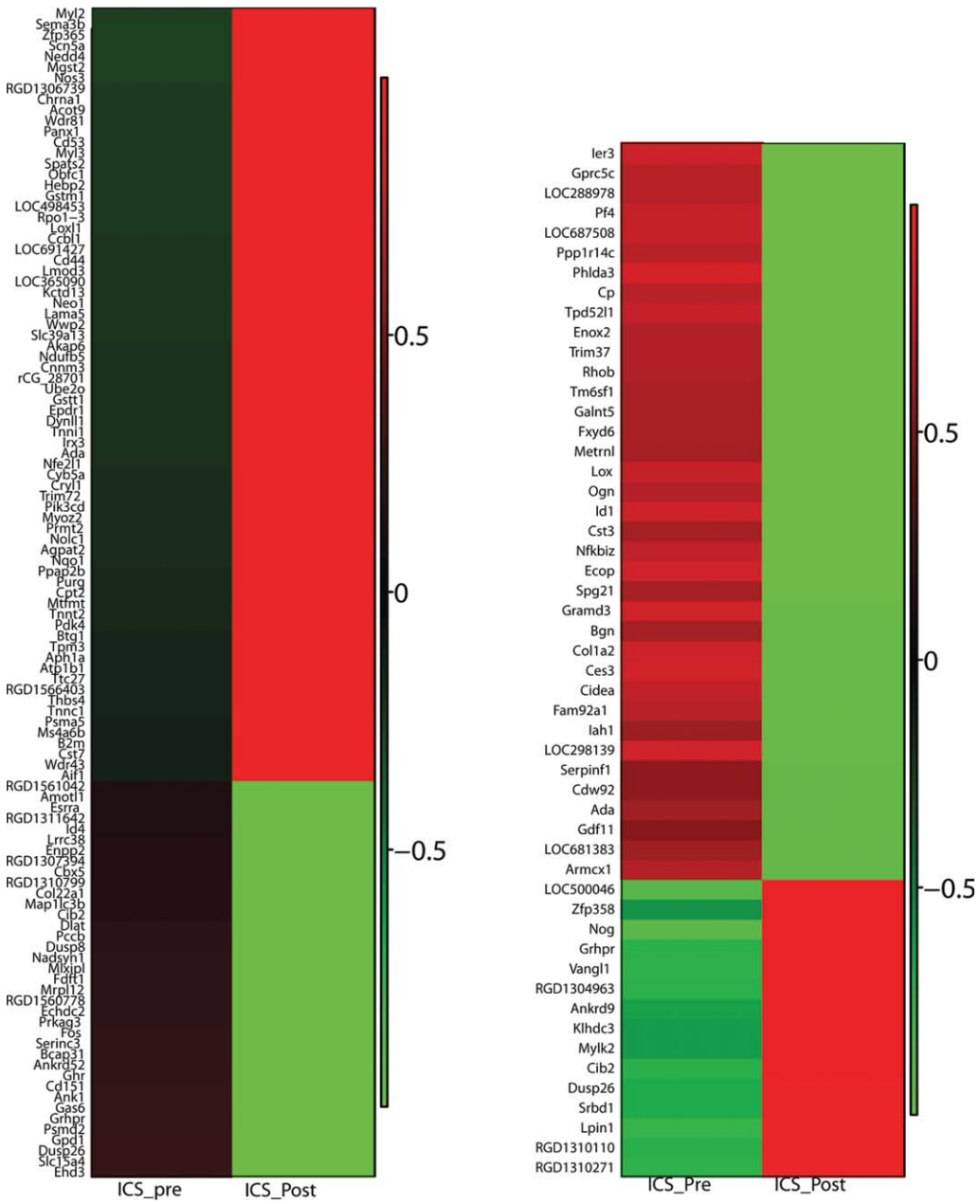

FIGURE 9. Heat map showing the correlation between differentially expressed genes with isometric contractile strength at **(a)** 1 week (left) and **(b)** 4 weeks after injection (right). Green represents negative correlation and red represents positive correlation.

with some differences, the transcriptional regulation observed in chemodenervated muscle after BoNT-A is similar to that seen in denervation models[28] and neuromuscular diseases,[29,30] with suppression of metabolism and muscle contraction, activation of atrophic pathways, and increased oxidative stress. We discuss the observed regulation in what follows, defining the "early" response, which is more complex, and the "late" response to neurotoxin.

Early Response to Botulinum Toxin Injection. ***Alterations in ECC and Sarcomeric Contraction.*** Reduced availability of ACh due to BoNT-A–impaired exocytosis causes increased expression of specific nAChRs, *Chrnd*, *Chrne*, embryonic *Chrng*, and especially *Chrna1*.[5] As previously reported, overexpression of *Chrng*, ordinarily undetectable in adult skeletal muscle, is a compensatory mechanism to create greater current flow, as it is localized along the entire length of the fiber.[31,32] Although our microarray did not capture *MuSK*, a crucial protein for nAChR clustering after BoNT-A[10] (upregulation confirmed through qPCR; see Fig. S2, online), *Lrp4* (a co-receptor for *Agrin*[33]) and *Rapsn* (required for clustering nAChRs on the postsynaptic membrane[34]) were upregulated significantly.

The observed upregulation of *Lrp4* and *Emb* may serve as a "retrograde signal" to stabilize the NMJ, facilitating formation of terminal sprouts and induction of nAChRs.[35,36]

Imbalance in ion flux after BoNT-A was reflected in the regulation of adult isoforms of K^+ gating channels such as *Kcnc1* and *Kcnab1*, and inwardly rectifying *Kcnj11*. Interestingly, strong upregulation of 2 non-adult voltage-gated Na^{2+}/K^+ ion channels, *Scn5a* (a cardiac isoform recently implicated in the occurrence of fibrillation potentials in denervated muscle fibers[37]) and *Kcnn3* (a K^+ channel implicated in fibrillation and hyperpolarization of denervated muscles[38,39]), suggests hyperexcitability of BoNT-A–injected muscle, analogous to denervated models. Reduced electrical activity also implies absence of an active need to maintain the Na^+/K^+ gradient, reducing the utility of certain Na^+/K^+ ion pumps, such as *Atp1b1* and *Atp1b2*.[40]

The transmission of neural excitation past the NMJ terminates at a specialized set of voltage sensors within the muscle T-system called dihydropyridine receptors (DHPRs), which are coupled mechanically to ryanodine receptors (RYRs) in the sarcoplasmic reticulum (SR). Downregulation of docking protein *Jph1* (which holds the T-system spatially close to the SR) suggests instability in the structural and spatial association between the SR and T-tubules at 1 week. Upregulation of *Cacnb1* (of the DHPR), *Fkbp1a*[41] (essential for minimizing Ca^{2+} leakage) in conjunction with the protracted and sustained upregulation of *Sln* (which inhibits the uptake of Ca^{2+} back into the SR) suggests increased availability of cytoplasmic Ca^{2+}, in contrast to denervated muscle.[42]

Genes that affect free Ca^{2+} dynamics, such as *Calm3*, calcineurin (*Ppp3cb/Ppp3ca*), and *Camk2a*, were clearly regulated. *Aqp4*, a water channel expressed at the sarcolemma of fast-twitch skeletal muscle, which has an expression that is altered in dystrophy and atrophy, was the single most strongly downregulated gene. Although the exact physiological role of *Aqp4* in skeletal muscle has yet to be defined, recent research on $Aqp4^{-/-}$ mice suggests it has a role in regulating the osmotic balance of muscle, affecting Ca^{2+} handling.[43] Taken together, these data suggest a lack of calcium homeostasis and impaired Ca^{2+} handling in BoNT-A–treated muscle, especially at 1 week after injection. These results are consistent with muscle responding to decreased neural activity.

The transmitted action potential in normal skeletal muscle is ultimately converted to mechanical contraction through physical coupling of several proteins within the muscle.[13] As expected, we observed suppression of several adult sarcomeric proteins of fast muscle. Downregulation of *Myoz1*, combined with upregulation of *Csrp3*,[28] suggests a shift in fiber composition at 1 week after BoNT-A treatment. This "mixed" state of expression beyond 1 week is further compounded by upregulation of genes expressing cardiac immature fiber isoforms, such as *Actc1*, *Myl6b*, and *Tnnt2*, with the largest increases occurring in the expression of *Myh3* and *Myh8*.

A disrupted state of the sarcolemma at 1 week is evidenced by downregulation of *Ank1*[44] (necessary to maintain integrity of network SR) along with upregulation of several other cytoskeletal proteins, *γFilamin*, *Sgc*, *Dmd*, *Dtna*, and *Dysf*. Overall, the observed activation of several mixed muscle isoforms points to activation of programs not seen in adult skeletal muscle, reinforcing the general idea that muscle injected with BoNT-A reverts to a more "immature" state in order to recover contractile function.

Reduced Metabolism and Impaired Mitochondrial Biogenesis. With BoNT-A–induced paralysis, there is reduced requirement for ATP consumption. Akin to denervation models,[28] we observed suppression of most genes involved in energy metabolism and production (via both oxidation of lipids and glycolysis), specifically at 1 week, which resolve by 4 weeks. As described in the Results section and in Figure 5, there is clear downregulation of enzymes involved in energy production via glycolysis, except for hexokinase (*Hk6*).

It has been reported previously in atrophy with preferential loss of fast muscle fibers that there is dramatic upregulation of *Ampd3*[45] (replenishes TCA-cycle intermediate substrates). Dramatic and prolonged upregulation of *Ampd3* in our study not only suggests an impaired TCA cycle, but further supports the idea of a shift in fiber composition. Another observation of BoNT-A–treated muscle is prolonged upregulation of *Scd1* (also validated using qPCR). Deficiency in Scd1, a rate-limiting enzyme that catalyzes the synthesis of monounsaturated fatty acid, has been correlated with increased oxygen consumption and subsequent β-oxidation in skeletal muscle.[46,47] Conversely, overexpression studies have shown decreased fatty acid oxidation, increased TAG synthesis, monosaturation of muscle fatty acids, and impaired glucose uptake and insulin signaling pathway.[48] The fact that it is upregulated until 12 weeks after injection leads us to speculate that *Scd1* may play a significant role in reduced energy production (via β oxidation) in addition to playing a role in reducing glucose uptake after BoNT-A injection.

Suppression of *Ckmt2* [outer mitochondrial membrane enzyme required for generating ATP

from phosphocreatine and adenosine diphosphate (ADP)] and *Ak1* (cytoplasmic enzyme that catalyzes generation of ATP from ADP) also points to reduced ATP turnover in injected muscle.

Upregulation of major energy/ATP availability sensors, AMPK $\alpha/\beta/\gamma$ (*Prkaa1*, *Prkag3*), point to reduced availability of ATP at 1 week. However, the targets of AMPK, the PPAR cofactors[49,50] *Ppargc1a* and *Ppargc1b*, known biomarkers of mitochondrial biogenesis in skeletal muscle, were downregulated,[51] suggesting possible stress-induced impairment of mitochondrial biogenesis.

Increased Oxidative Stress and Metal Ion Imbalance. Denervation and immobilization studies have demonstrated repeatedly that one of the causes of atrophy is increased accumulation of ROS and trace metals in skeletal muscle.[52–54] In that same vein, we observed transcriptional activation of several oxidative stress markers implicated in atrophy, such as the metallothioneins (Mt1a, Mt2a).[45,55] Most striking, however, was the increase in the various isoforms of glutathione *S*-transferase, including *Gstm1* and *Gstt2*, as a compensatory response to increased production of ROS or oxidative stress.[56] Interestingly, however, the mitochondrial ROS scavenger superoxide dismutase 2 (*Sod2*) was downregulated and may have been confounded by mitochondrial dysfunction.

Imbalance of metal ion concentration has been reported previously in studies of immobilization and disuse.[57] Zinc ion homeostasis has been linked closely to a redox state of cells in various tissues.[58] We observed significant upregulation of zinc SLCs (*Slc30a2*, *Slc30a4*), which are suggested to confer a cytoprotective effort by preventing cells from free Zn ion toxicity.[59] Although the exact physiological role of Zn ion toxicity in chemodenervated muscle is not understood fully, we hypothesize that the observed upregulation of these transporters in conjunction with increased expression of metallothioneins suggests a metal ion imbalance that may contribute to BoNT-A–induced atrophy of muscle.

Competing Pathways Contributing to Concomitant Atrophy and Recovery of Skeletal Muscle. Atrophy and consequent muscle loss in skeletal muscle can occur through activation of the NF-κB signaling pathway (*Traf2*, *Nfkb2*, and *Nfkbie*, and positive activators *Ascc2* and *Litaf*) along with activation of the TGF-β pathway.[60] Loss of muscle mass has been attributed to accelerated proteolytic degradation of the contractile apparatus through deployment of factors such as *Capn2*, *Ctsl1*, and *Casp3*,[61] and eventual degradation of the fragmented actin–myosin complexes through the ubiquitin-proteasomal system. Similar to denervation studies, but in contrast to neuromuscular diseases,[29,30] activation of atrophy markers, *Atrogin1/MAFbx* (*Fbxo32*) and *Trim63* (*MuRF1*), 2 muscle-specific ubiquitin ligases downstream of the NF-κB pathway, is observed after BoNT-A treatment.[11,62]

Several studies have demonstrated the role of TGF-β signaling in atrophying skeletal muscle and the powerful role of TGF-β family growth factors such as myostatin (*Mstn*) in regulating muscle size.[63] Although differential regulation of *Mstn* was not observed in our study, follistatin (*Fst*),[64] a myostatin inhibitor, was upregulated significantly. This, along with the repression of *Acvr2b*, a transmembrane activin receptor of *Mstn*, points to inhibition of the pro-atrophic action of *Mstn* in injected muscle. Upregulation of early-response genes downstream of *Tgfb1*, including *Junb* and *Fos* along with small GTPases *RhoA* and *RhoC* and its inhibitors (*Smad7* and *Fkbp1a*), further emphasizes the conflicting signaling of muscle treated with BoNT-A. In contrast to ATPases, such as *Atp1b1* and *Atp1b2*, *Atp1b4*, has been shown to localize to intracellular stores, predominantly the inner myonuclear membrane, in perinatal skeletal muscle of placental mammals and to regulate TGF-β signaling in skeletal muscle. Although no direct evidence of its localization patterns exists, we hypothesize that prolonged upregulation of *Atp1b4* (validated via qPCR) may be contributing to similar functions in BoNT-A–treated muscle.

Insulin-like growth factors (IGFs) and their role in upregulation of nAChRs, muscle growth,[69,70] and their metabolic effects, have been studied extensively. The observed regulation of IGF binding proteins, such as *Igfbp5* (inhibits action of *Igf1* by sequestering it to the ECM[67] and suppresses nerve sprouting[7]), is consistent with previous studies of BoNT-A treatment.[11] Although we found no significant regulation of *Igf1*, upregulation of its receptor, *Igf1r*, may compensate for the decreased availability of *Igf1*. Activation of *Igf1r* results in phosphorylation of insulin receptor substrates (*Irs1*) and regulation of several downstream players such as *Akt1*, *Pik3* (*Pik3r4*), and the energy/ATP availability sensor AMPK $\alpha/\beta/\gamma$. The observed spike in *Igf2* at 4 weeks correlates with studies showing a preferential spike in *Igf2* nearly 20 days after denervation/nerve injury.[65]

Although the exact role of myogenic regulatory factors[68] (MRFs) in differentiated post-mitotic skeletal muscle is not understood fully, the observed upregulation of *MyoD*, *Myog*, and *Mrf4/Myf6* may reflect satellite cell activation.[69] These factors may be necessary for activating transcriptional programs required for recovery of muscle function, such as *Ankrd1*. Concomitant with activation of MRFs, there is upregulation of several cell-cycle control genes known to play a role in satellite cell proliferation, such as *Tp53*, *Pcna*, *Myc*, and cyclin-

dependent kinase inhibitors *Cdkn1a* (suggested to confer a protective, anti-apoptotic effect[70]) and *Cdkn1c*. *Gadd45a*, a marker for atrophy also involved in cell-cycle control has been identified repeatedly as being overexpressed in models of denervation/chemodenervation.[10,11,28] Recent reports have indicated that the pro-atrophy transcription factor *Atf4* may induce expression of *Gadd45a* in muscles subject to 3 distinct skeletal muscle stresses of fasting, immobilization, and denervation.[71] Its expression was shown to be necessary but not sufficient for expression of *Gadd45a*. However, we observed a conflicting program of regulation in our data with *Atf4* being downregulated, suggesting alternate roles for *Atf4* and regulation of *Gadd45a* in BoNT-A–treated muscle at 1 week.

Further regulatory conflicts occur through upregulation at 1 week of 4 inhibitors of DNA binding genes (*Id1*, *Id2*, *Id3*, and *Id4*), which have been shown to inhibit muscle growth and differentiation.[72] Reduced contractile activity leads to a reduction in signaling that promotes muscle growth but inhibits complete fiber death (autophagy) triggered through pathways such as *Pik3/Akt*[73] and activation of runt transcription factor (*Runx1*). *Runx1* has been shown to sustain muscle[26] under atrophic conditions by inducing expression of genes required for muscle growth and function (*Myh2*, *Scn5a*, *Rrad*, *Myh3*, and *Chrng*) and repressing atrophy genes (*Gadd45a* and *Aqp4*).

Later Response to Botulinum Toxin Injection. Importantly, we found that, by 4 weeks, the transcriptional events leading to muscle atrophy and weakness were essentially completed. Although the functional properties of muscle are highly impaired at this time-point, the transcriptional response is essentially complete and is in the process of recovering. This is clearly seen by the fact that, of the 1989 genes regulated after injection, only 231 were actually still changing after 4 weeks.

Recovering NMJ, Sustained Oxidative Stress, and Lack of Ca^{2+} Homeostasis. Although the muscle slows down transcriptionally, the expression of certain pathways is still significant at 4 weeks. In contrast to other genes of the NMJ, *Emb* and *Chrna1* were upregulated up to 12 weeks, with significant remodeling of the synaptic basal lamina (*Lama5*, *Col4a5*, and *Nid2* upregulated) at 4 weeks. *Nid2*, involved in synapse maintenance[74] is associated selectively with the synaptic basal lamina at the NMJ. Taken together, these findings suggest reinnervation and a continuing effort by muscle toward stabilization of the NMJ at 4 weeks.

Upregulation of the SR calcium-sequestering protein *Casq2* suggests an effort by muscle to maintain Ca^{2+} within the SR, possibly counteracting continued overactivation of *Sln*. Interestingly, we found strong upregulation of a calmodulin-like protein called *Calml3* beginning at 4 weeks. Although its exact function is not yet determined in skeletal muscle, it is known to compete with calmodulin in other tissues, further suggesting alterations in the Ca^{2+} handling properties of muscle.[75] Upregulation of certain transcription regulators of atrophy and growth, such as *Myod1*, *Id1*, *Id3*, *Runx1*, *Gadd45a*, *Cdkn1a*, and *Cdkn1c*, was observed until 4 weeks.

ECM Remodeling and Fibrosis. The most pronounced effect at 4 weeks was active remodeling of the ECM and possibly even fibrosis. ECM production is regulated in part by activation of several targets of TGF-β, including *Ctgf* and *Ltbp1*. Upregulation of early growth response (*Egr-1*), a zinc-finger transcription factor known to regulate collagen expression (particularly *Col1a2*) in response to TGF-β[76] and act downstream of multiple pro-fibrotic agents to regulate transcription, was observed. The persistent activation of these genes in conjunction with dramatic upregulation of ECM genes beyond 1 week (see Results and Fig. S1, online) leads us to propose activation of similar fibrotic programs by 4 weeks after BoNT-A injection, resulting in fibrosis of injected tissue. This also emphasizes the possibility of a multifaceted role of *Igfbp5* after BoNT-A injection.[77–79]

Significant regulation of *Scd1*, *Sln*, *Cdkn1a*, *Cdkn1c*, and *S100a4* beyond 4 weeks suggested incomplete recovery of muscle, even 4 weeks after treatment. Importantly, we observed no biologically significant changes, at least transcriptionally, in skeletal muscle treated with BoNT-A at 52 weeks after injection.

In conclusion, this analysis provides a global assessment of changes occurring in BoNT-A–treated muscle over a period of 1 year. By utilizing previously described physiological networks of muscle, we provided a systems-level analysis that categorically assesses expression changes after BoNT-A treatment. Dramatic transcriptional regulation in several of these networks was evident at week 1, leading to derangement of the ECM and fibrillar components by week 4. The shift toward expression of slow and immature isoforms emulating "immature" muscle possibly aids in muscle recovery. It should be noted that, although this is a transcriptional expression study, the data have clinical relevance. Specifically, they indicate that, at the molecular level, the effects of BoNT-A are relatively rapid, because most transcripts returned to control levels within 4 weeks. This is consistent with the use of the term "reversible chemodenervation," often used with reference to the action of BoNT-A. It is also of interest to note that, in spite of the

relatively fast transcriptional response, the structural and functional response lags somewhat. This is probably a function of the length of time required for a neuromuscular unit to recover from a period of denervation-induced atrophy and fibrosis. Transcriptional regulation associated with atrophy and fibrosis suggests the possibility of transient extracellular effects after BoNT-A injection. Although no long-term transcriptional abnormalities were observed, further studies are necessary to determine optimal intervals for BoNT-A treatment from both a biological and physiological point of view.

REFERENCES

1. McLaughlin JF, Bjornson KF, Astley SJ, Graubert C, Hays RM, Roberts TS, et *al.* Selective dorsal rhizotomy: efficacy and safety in an investigator-masked randomized clinical trial. Dev Med Neurol 1998; 40:220–232.
2. Koman LA, Mooney JF III, Smith BP, Walker F, Leon JM. Botulinum toxin type A neuromuscular blockade in the treatment of lower extremity spasticity in cerebral palsy: a randomized, double-blind, placebo-controlled trial. J Pediatr Orthop 2000;20:108.
3. Truong DD, Stenner A, Reichel G. Current clinical applications of botulinum toxin. Curr Pharm Des 2009;15:3671–3680.
4. Dolly JO, Lawrence GW, Meng J, Wang J, Ovsepian SV. Neuro-exocytosis: botulinum toxins as inhibitory probes and versatile therapeutics. Curr Opin Pharmacol 2009;9:326–335.
5. Simpson LL. Identification of the major steps in botulinum toxin action. Annu Rev Pharmacol Toxicol 2004;44:167–193.
6. .De Paiva A, Meunier FA, Molgó J, Aoki KR, Dolly JO. Functional repair of motor endplates after botulinum neurotoxin type A poisoning: biphasic switch of synaptic activity between nerve sprouts and their parent terminals. Proc Natl Acad Sci 1999;96:3200–3205.
7. Meunier FA, Schiavo G, Molgó J. Botulinum neurotoxins: from paralysis to recovery of functional neuromuscular transmission. J Physiol Paris 2002;96:105–113.
8. Duchen LW. Changes in the electron microscopic structure of slow and fast skeletal muscle fibres of the mouse after the local injection of botulinum toxin. J Neurol Sci 1971;14:61–74.
9. Lebeda FJ, Cer RZ, Stephens RM, Mudunuri U. Temporal characteristics of botulinum neurotoxin therapy. Expert Rev Neurother 2010; 10:93–103.
10. Ma J, Elsaidi GA, Smith TL, Walker FO, Tan KH, Martin E, et *al.* Time course of recovery of juvenile skeletal muscle after botulinum toxin A injection: an animal model study. Am J Phys Med Rehabil 2004;83:774–780.
11. Shen J, Ma J, Lee C, Smith BP, Smith TL, Tan KH, et *al.* How muscles recover from paresis and atrophy after intramuscular injection of botulinum toxin A: study in juvenile rats. J Orthop Res 2006; 24:1128–1135.
12. Smith LR, Meyer G, Lieber RL. Systems analysis of biological networks in skeletal muscle function. Wiley Interdiscip Rev Syst Biol Med 2013;5:55–71.
13. Wang Y, Winters J, Subramaniam S. Functional classification of skeletal muscle networks. I. Normal physiology. J Appl Physiol 2012;113: 1884–1901.
14. Minamoto VB, Hulst JB, Lim M, Peace WJ, Bremner SN, Ward SR, et *al.* Increased efficacy and decreased systemic effects—effects of botulinum A toxin injection after passive muscle manipulation. Dev Med Child Neurol 2007;49:907–914.
15. Edwards CA, O'Brien WD. Modified assay for determination of hydroxyproline in a tissue hydrolyzate. Clin Chim Acta 1980;104:161–167.
16. Schmittgen TD, Livak KJ. Analyzing real-time PCR data by the comparative CT method. Nat Protoc 2008;3:1101–1108.
17. R Development C. TEAM: R: A language and environment for statistical computing. Vienna, Austria: R Foundation for Statistical Computing; 2011.
18. Gentleman RC, Carey VJ, Bates DM, Bolstad B, Dettling M, Dudoit S, et *al.* Bioconductor: open software development for computational biology and bioinformatics. Genome Biol 2004;5:R80.
19. Wu Z, Irizarry RA, Gentleman R, Murillo FM, Spencer F. A model based background adjustment for oligonucleotide expression arrays. J Am Stat Assoc 2004;99:909–917.
20. Barrett T, Wilhite SE, Ledoux P, Evangelista C, Kim IF, Tomashevsky M, et *al.* NCBI GEO: archive for functional genomics data sets—update. Nucleic Acids Res 2013;41:D991–D995.
21. Langfelder P, Horvath S. WGCNA: an R package for weighted correlation network analysis. BMC Bioinformatics 2008;9:559.
22. Kayala MA, Baldi P. Cyber-T web server: differential analysis of high-throughput data. Nucleic Acids Res 2012;40:W553–W559.
23. Goodman MN, Dluz SM, McElaney MA, Belur E, Ruderman NB. Glucose uptake and insulin sensitivity in rat muscle: changes during 3–96 weeks of age. Am J Physiol Endocrinol Metab 1983;244:E93–E100.
24. Piec I, Listrat A, Alliot J, Chambon C, Taylor RG, Bechet D. Differential proteome analysis of aging in rat skeletal muscle. FASEB J 2005; 19:1143–1145.
25. Huang DW, Sherman BT, Lempicki RA. Systematic and integrative analysis of large gene lists using DAVID bioinformatics resources. Nat Protoc 2008;4:44–57.
26. Wang X, Blagden C, Fan J, Nowak SJ, Taniuchi I, Littman DR, et *al.* Runx1 prevents wasting, myofibrillar disorganization, and autophagy of skeletal muscle. Sci Signal 2005;19:1715.
27. Mann CJ, Perdiguero E, Kharraz Y, Aguilar S, Pessina P, Serrano AL, et *al.* Aberrant repair and fibrosis development in skeletal muscle. Skelet Muscle 2011;1:21.
28. Raffaello A, Laveder P, Romualdi C, Bean C, Toniolo L, Germinario E, et *al.* Denervation in murine fast-twitch muscle: short-term physiological changes and temporal expression profiling. Physiol Genomics 2006;25:60–74.
29. Millino C, Fanin M, Vettori A, Laveder P, Mostacciuolo ML, Angelini C, et *al.* Different atrophy–hypertrophy transcription pathways in muscles affected by severe and mild spinal muscular atrophy. BMC Med 2009;7:14.
30. Mo K, Razak Z, Rao P, Yu Z, Adachi H, Katsuno M, et *al.* Microarray analysis of gene expression by skeletal muscle of three mouse models of Kennedy disease/spinal bulbar muscular atrophy. PloS One 2010; 5:e12922.
31. Numberger M, Dürr I, Kues W, Koenen M, Witzemann V. Different mechanisms regulate muscle-specific AChR gamma-and epsilon-subunit gene expression. EMBO J 1991;10:2957.
32. Witzemann V, Brenner HR, Sakmann B. Neural factors regulate AChR subunit mRNAs at rat neuromuscular synapses. J Cell Biol 1991;114:125–141.
33. Kim N, Stiegler AL, Cameron TO, Hallock PT, Gomez AM, Huang JH, et *al.* Lrp4 is a receptor for Agrin and forms a complex with MuSK. Cell 2008;135:334–342.
34. Goodsell DS. Neuromuscular synapse. Biochem Mol Biol Educ 2009; 37:204–210.
35. Lain E, Carnejac S, Escher P, Wilson MC, Lømo T, Gajendran N, et *al.* A novel role for embigin to promote sprouting of motor nerve terminals at the neuromuscular junction. J Biol Chem 2009;284: 8930–8939.
36. Yumoto N, Kim N, Burden SJ. Lrp4 is a retrograde signal for presynaptic differentiation at neuromuscular synapses. Nature 2012;489: 438–442.
37. Sekiguchi K, Kanda F, Mitsui S, Kohara N, Chihara K. Fibrillation potentials of denervated rat skeletal muscle are associated with expression of cardiac-type voltage-gated sodium channel isoform Nav1.5. Clin Neurophysiol 2012;123:1650–1655.
38. Kostrominova TY, Dow DE, Dennis RG, Miller RA, Faulkner JA. Comparison of gene expression of 2-mo denervated, 2-mo stimulated-denervated, and control rat skeletal muscles. Physiol Genomics 2005; 22:227–243.
39. Kimura T, Takahashi MP, Fujimura H, Sakoda S. Expression and distribution of a small-conductance calcium-activated potassium channel (SK3) protein in skeletal muscles from myotonic muscular dystrophy patients and congenital myotonic mice. Neurosci Lett 2003;347:191–195.
40. Hundal HS, Marette A, Ramlal T, Liu Z, Klip A. Expression of β subunit isoforms of the Na+,K+-ATPase is muscle type-specific. FEBS Lett 1993;328:253–258.
41. Engel A, Franzini-Armstrong C. Myology: basic and clinical. New York: McGraw-Hill; 2004.
42. Midrio M. The denervated muscle: facts and hypotheses. A historical review. Eur J Appl Physiol 2006;98:1–21.
43. Basco D, Nicchia GP, D'Alessandro A, Zolla L, Svelto M, Frigeri A. Absence of aquaporin-4 in skeletal muscle alters proteins involved in bioenergetic pathways and calcium handling. PloS One 2011;6: e19225.
44. Ackermann MA, Ziman AP, Strong J, Zhang Y, Hartford AK, Ward CW, et *al.* Integrity of the network sarcoplasmic reticulum in skeletal muscle requires small ankyrin 1. J Cell Sci 2011;124:3619–3630.
45. Lecker SH, Jagoe RT, Gilbert A, Gomes M, Baracos V, Bailey J, et *al.* Multiple types of skeletal muscle atrophy involve a common program of changes in gene expression. FASEB J 2004;18:39–51.
46. Dobrzyn A, Dobrzyn P. Stearoyl-CoA desaturase—a new player in skeletal muscle metabolism regulation. J Physiol Pharmacol 2006; 57(suppl 10):31–42.
47. Dobrzyn A, Ntambi JM. The role of stearoyl-CoA desaturase in the control of metabolism. Prostagland Leukot Essent Fatty Acids 2005; 73:35–41.

48. Voss M, Beha A, Tennagels N, Tschank G, Herling A, Quint M, et *al.* Gene expression profiling in skeletal muscle of Zucker diabetic fatty rats: implications for a role of stearoyl-CoA desaturase 1 in insulin resistance. Diabetologia 2005;48:2622–2630.
49. Cantó C, Gerhart-Hines Z, Feige JN, Lagouge M, Noriega L, Milne JC, et *al.* AMPK regulates energy expenditure by modulating NAD+ metabolism and SIRT1 activity. Nature 2009;458:1056–1060.
50. Bouzakri K, Zachrisson A, Al-Khalili L, Zhang BB, Koistinen HA, Krook A, et *al.* siRNA-based gene silencing reveals specialized roles of IRS-1/Akt2 and IRS-2/Akt1 in glucose and lipid metabolism in human skeletal muscle. Cell Metab 2006;4:89–96.
51. Olesen J, Kiilerich K, Pilegaard H. PGC-1α-mediated adaptations in skeletal muscle. Pflugers Arch Eur J Physiol 2010;460:153–162.
52. O'Leary MF, Hood DA. Denervation-induced oxidative stress and autophagy signaling in muscle. Autophagy 2009;5:230–231.
53. Abruzzo PM, di Tullio S, Marchionni C, Belia S, Fanó G, Zampieri S, et *al.* Oxidative stress in the denervated muscle. Free Radic Res 2010; 44:563–576.
54. Kondo H, Miura M, Itokawa Y. Oxidative stress in skeletal muscle atrophied by immobiLization. Acta Physiol Scand 1991;142:527–528.
55. Muller FL, Song W, Jang YC, Liu Y, Sabia M, Richardson A, et *al.* Denervation-induced skeletal muscle atrophy is associated with increased mitochondrial ROS production. Am J Physiol Regul Integr Comp Physiol 2007;293:R1159–R1168.
56. Reid M, Jahoor F. Glutathione in disease. Curr Opin Clin Nutr Metab Care 2001;4:65–71.
57. Kondo H, Miura M, Nakagaki I, Sasaki S, Itokawa Y. Trace element movement and oxidative stress in skeletal muscle atrophied by immobilization. Am J Physiol Endocrinol Metab 1992;262:E583–E590.
58. Maret W, Krężel A. Cellular zinc and redox buffering capacity of metallothionein/thionein in health and disease. Mol Med 2007;13: 371.
59. Maret W. Metallothionein redox biology in the cytoprotective and cytotoxic functions of zinc. Exp Gerontol 2008;43:363–369.
60. Jackman RW, Kandarian SC. The molecular basis of skeletal muscle atrophy. Am J Physiol Cell Physiol 2004;287:C834–C843.
61. Plant PJ, Bain JR, Correa JE, Woo M, Batt J. Absence of caspase-3 protects against denervation-induced skeletal muscle atrophy. J Appl Physiol 2009;107:224–234.
62. Bodine SC, Latres E, Baumhueter S, Lai VK-M, Nunez L, Clarke BA, et *al.* Identification of ubiquitin ligases required for skeletal muscle atrophy. Sci Signal 2001;294:1704.
63. Kollias HD, McDermott JC. Transforming growth factor-β and myostatin signaling in skeletal muscle. J Appl Physiol 2008;104:579–587.
64. Amthor H, Nicholas G, McKinnell I, Kemp CF, Sharma M, Kambadur R, et *al.* Follistatin complexes myostatin and antagonises myostatin-mediated inhibition of myogenesis. Dev Biol 2004;270: 19–30.
65. Sullivan KA, Kim B, Feldman EL. Insulin-like growth factors in the peripheral nervous system. Endocrinology 2008;149:5963–5971.
66. Sacheck JM, Ohtsuka A, McLary SC, Goldberg AL. IGF-I stimulates muscle growth by suppressing protein breakdown and expression of atrophy-related ubiquitin ligases, atrogin-1 and MuRF1. Am J Physiol Endocrinol Metab 2004;287:E591–E601.
67. Schneider MR, Wolf E, Hoeflich A, Lahm H. IGF-binding protein-5: flexible player in the IGF system and effector on its own. J Endocrinol 2002;172:423–440.
68. Sabourin LA, Rudnicki MA. The molecular regulation of myogenesis. Clin Genet 2000;57:16–25.
69. Chen C-M, Stott NS, Smith HK. Effects of botulinum toxin A injection and exercise on the growth of juvenile rat gastrocnemius muscle. J Appl Physiol 2002;93:1437–1447.
70. Walsh K, Perlman H. Cell cycle exit upon myogenic differentiation. Curr Opin Genet Dev 1997;7:597–602.
71. Ebert SM, Dyle MC, Kunkel SD, Bullard SA, Bongers KS, Fox DK, et *al.* Stress-induced skeletal muscle Gadd45a expression reprograms myonuclei and causes muscle atrophy. J Biol Chem 2012;287:27290–27301.
72. Jen Y, Weintraub H, Benezra R. Overexpression of Id protein inhibits the muscle differentiation program: in vivo association of Id with E2A proteins. Genes Dev 1992;6:1466–1479.
73. Stitt TN, Drujan D, Clarke BA, Panaro F, Timofeyva Y, Kline WO, et *al.* The IGF-1/PI3K/Akt pathway prevents expression of muscle atrophy-induced ubiquitin ligases by inhibiting FOXO transcription factors. Mol Cell 2004;14:395–403.
74. Fox MA, Ho MS, Smyth N, Sanes JR. A synaptic nidogen: developmental regulation and role of nidogen-2 at the neuromuscular junction. Neural Devel 2008;3:1–17.
75. Bennett RD, Mauer AS, Pittelkow MR, Strehler EE. Calmodulin-like protein upregulates myosin-10 in human keratinocytes and is regulated during epidermal wound healing in vivo. J Invest Dermatol 2008;129:765–769.
76. Chen S-J, Ning H, Ishida W, Sodin-Semrl S, Takagawa S, Mori Y, et *al.* The early-immediate gene EGR-1 is induced by transforming growth factor-β and mediates stimulation of collagen gene expression. J Biol Chem 2006;281:21183–21197.
77. Sureshbabu A, Okajima H, Yamanaka D, Shastri S, Tonner E, Rae C, et *al.* IGFBP-5 induces epithelial and fibroblast responses consistent with the fibrotic response. Biochem Soc Trans 2009;37:882.
78. Sureshbabu A, Tonner E, Allan GJ, Flint DJ. Relative roles of TGF-β and IGFBP-5 in idiopathic pulmonary fibrosis. Pulm Med 2011;2011.
79. Yasuoka H, Hsu E, Ruiz XD, Steinman RA, Choi AM, Feghali-Bostwick CA. The fibrotic phenotype induced by IGFBP-5 is regulated by MAPK activation and egr-1-dependent and -independent mechanisms. Am J Pathol 2009;175:605–615.